

Disorder effects at a nematic quantum critical point in d -wave cuprate superconductor

Jing Wang,¹ Guo-Zhu Liu,^{1,2} and Hagen Kleinert²

¹*Department of Modern Physics, University of Science and Technology of China, Hefei, Anhui, 230026, P.R. China*

²*Institut für Theoretische Physik, Freie Universität Berlin, Arnimallee 14, D-14195 Berlin, Germany*

A d -wave high temperature cuprate superconductor exhibits a nematic ordering transition at zero temperature. Near the quantum critical point, the coupling between gapless nodal quasiparticles and nematic order parameter fluctuation can result in unusual behaviors, such as extreme anisotropy of fermion velocities. We study the disorder effects on the nematic quantum critical behavior and especially on the flow of fermion velocities. The disorders that couple to nodal quasiparticles are divided into three types: random mass, random gauge field, and random chemical potential. A renormalization group analysis shows that random mass and random gauge field are both irrelevant and thus do not change the fixed point of extreme velocity anisotropy. However, the marginal interaction due to random chemical potential destroys this fixed point and makes the nematic phase transition unstable.

PACS numbers: 73.43.Nq, 74.72.-h, 74.25.Dw

I. INTRODUCTION

One important reason that high-temperature cuprate superconductors are hard to understand is that they have very complicated phase diagram. The competitions and transitions between different phases give rise to many unusual properties, and hence have attracted considerable theoretical and experimental efforts in the past two decades. Among the widely studied competing orders, the various phase of the anisotropic electronic liquid are of particular interests. Kivelson, Fradkin, and Emery proposed that due to the local electronic phase separation, a number of novel electronic liquid crystal phases can exist in a doped Mott insulator [1]. The simplest of such phases is the electronic nematic phase, in which the rotational symmetry is broken but the translational symmetry is preserved. In recent years, the nematic ordering phase transition has been investigated extensively [2, 3]. The resistivity anisotropy observed by Ando *et al.* in two types of cuprate superconductors provided the early evidence for the predicted nematic phase [4]. More recently, the neutron-scattering experiments performed in $\text{YBa}_2\text{Cu}_3\text{O}_{6.45}$ also pointed to the existence of nematic phase [5]. Further evidences came from the observed in-plane anisotropy of the Nernst effect in the pseudogap region of $\text{YBa}_2\text{Cu}_3\text{O}_y$ [6] and from the scanning tunneling microscopy experiments performed in the pseudogap region of $\text{Bi}_2\text{Sr}_2\text{CaCu}_2\text{O}_{8+\delta}$ [7]. Interestingly, there are also compelling experimental indications for the existence of nematic phase in $\text{Sr}_3\text{Ru}_2\text{O}_7$ [8] and in newly discovered iron-based superconductor [9].

In the language of field theory, the nematic phase has an Ising-type order parameter that can be represented by a real scalar field ϕ . However, the dynamics of the system close to the critical point can not be fully described by an effective ϕ^4 theory [10] when there are itinerant electrons. The interaction between quantum fluctuation of the nematic order parameter and the itinerant electrons has to be treated carefully. Close to the quantum critical point, this interaction becomes singular, which was

shown to be able to produce highly unusual, non-Fermi liquid like, behaviors [11–14]. The nematic physics is intimately related to Pomeranchuk instability and has also been investigated from this point of view [15, 16].

Besides the pseudogap phase of underdoped cuprates, it is also interesting to study the nematic transition that occurs in the d -wave superconducting phase [17–21]. This is a new example of quantum phase transitions happening in the superconducting dome [22–24], which is a widely studied topic. In the superconducting phase, the nematic order parameter interacts strongly with the gapless nodal quasiparticles, which are the low-energy excitations of a d -wave superconductor. This interaction remarkably affects the dynamics of both nodal quasiparticles and nematic order parameter. An early work of Vojta *et al.* [17] presented a detailed renormalization group (RG) analysis of various types of Yukawa couplings in the d -wave superconducting phase, including nematic type coupling. More recently, Kim *et al.* studied the effect of quantum fluctuations of nematic order parameter on the spectral properties of nodal quasiparticles [18].

In actual d -wave cuprate superconductor, the gapless nodal quasiparticles have a Fermi velocity v_F and a gap velocity v_Δ , which are not equal. Indeed, the ratio v_Δ/v_F may be as small as 1/20 [25]. This small ratio plays an important role because it appears in a number of observable quantities [25]. For instance, it was found [26] that the dc thermal conductivity contains the large inverse of this ratio as

$$\frac{\kappa}{T} \propto \frac{k_B^2}{\hbar} \left(\frac{v_\Delta}{v_F} + \frac{v_F}{v_\Delta} \right) \quad (1)$$

at nearly zero temperature. This easily accessible material property is universal — it is independent of the amount of disorder [26]. This universality was confirmed by transport measurements [27]. Since the inverse of v_Δ/v_F is so large it completely dominates κ/T .

An interesting problem is how the velocity ratio is influenced by the nematic phase transition. Recently, Huh and Sachdev [19] studied this problem by making a care-

ful RG analysis within an effective field theory of nematic ordering transition. They found that v_Δ/v_F flows to a fixed point with $v_\Delta/v_F \rightarrow 0$, i.e., the inverse velocity ratio v_F/v_Δ diverges. Therefore, the nematic ordering transition in d -wave superconductor is accompanied by the appearance of an extreme velocity anisotropy. Since the diverging velocity ratio v_F/v_Δ enters various physical properties, the predicted extreme anisotropy should have observable effects. In particular, the low-temperature dc thermal conductivity is expected to be significantly enhanced near the critical point. By using a Boltzmann equation approach, Fritz and Sachdev [21] calculated the thermal conductivity enhancement near the nematic quantum critical point due to the divergence of v_F/v_Δ . If this enhancement were observed in transport experiments at certain doping concentration, this would serve as an important evidence for the existence of nematic transition in d -wave cuprate superconductor.

When studying the low-temperature transport properties of an interacting electron system, it is hardly possible to ignore the disorder effects. First of all, the fermions are always scattered by certain amount of disorder in any realistic physical system. Moreover, although the elastic scattering due to quenched disorder is less important at high temperature, it dominates over the inelastic scattering due to inter-particle interactions at very low temperature. The disorder effects should be taken into account when calculating the low-temperature thermal conductivity. The nematic order parameter fluctuation can lead to significant enhancement of thermal conductivity only when the fixed point of extreme velocity anisotropy is stable against disorder scattering. If the fixed point is changed or even destroyed by disorder, the thermal conductivity enhancement will not occur in practice. It is therefore crucial to examine the disorder effects on the RG flow of fermion velocities, especially on the stability of extreme anisotropy of velocities.

In general, the disorders coupled to gapless nodal quasiparticles in d -wave superconductor can be divided into three types: random chemical potential, random gauge field, and random mass. The difference comes from the different Pauli matrices used to define the fermion-disorder interacting terms. The effects of these disorders on the low-temperature transport properties of nodal quasiparticles have been discussed extensively [28, 29]. These disorders will alter the RG flows of fermion velocities. On the other hand, the RG flow of strength parameters of fermion-disorder couplings are determined by fermion velocities, and thus should be calculated self-consistently with the flow of fermion velocities.

In this paper, we present a RG analysis of the interplay between nematic order parameter fluctuation and disorder scattering. We derive a series of coupled RG equations of fermion Fermi velocity v_F , gap velocity v_Δ , and disorder strength parameter g . In the cases of random mass and random gauge field, the corresponding disorder strength parameters both flow to zero at low energy. Therefore, these two kinds of disorders do not

change the flow of fermion velocities and hence the fixed point of extreme velocity anisotropy is stable. However, the strength parameter of random chemical potential remains a constant even down to the lowest energy, and thus is able to modify the fermion velocities significantly. We found that the fermion velocities do not flow to any fixed points, but indeed oscillate rapidly between positive and unphysical negative values. This implies that the extreme anisotropy fixed point is destroyed and the nematic phase transition may become unstable due to random chemical potential.

In Sec. II, we define the model action in the presence of both nematic order parameter fluctuation and disorder. In Sec. III, we calculate the fermion self-energy corrections due to nematic order parameter and disorder scattering. The fermion-disorder vertex corrections due to nematic and disorder interactions are also computed in this section. In Sec. IV, we make the RG analysis and obtain the self-consistent RG equations for fermion velocities and disorder strength parameter. These equations are solved both analytically and numerically in Sec. V. From the solutions, we found that the fixed point of extreme velocity anisotropy is not changed by random mass and random gauge field. However, the random chemical potential destroys this fixed point and indeed makes the nematic phase transition unstable. In Sec. VI, we briefly summarize the results obtained in this paper and discuss the possible experimental detection of the predicted extreme velocity anisotropy.

II. MODEL

We start from the following action

$$S = S_\psi + S_\phi + S_{\psi\phi}, \quad (2)$$

where the free action for nodal quasiparticles is

$$S_\psi = \int \frac{d^2\mathbf{k}}{(2\pi)^2} \frac{d\omega}{2\pi} \psi_{1a}^\dagger (-i\omega + v_F k_x \tau^z + v_\Delta k_y \tau^x) \psi_{1a} \\ + \int \frac{d^2\mathbf{k}}{(2\pi)^2} \frac{d\omega}{2\pi} \psi_{2a}^\dagger (-i\omega + v_F k_y \tau^z + v_\Delta k_x \tau^x) \psi_{2a}, \quad (3)$$

where $\tau^{(x,y,z)}$ denote Pauli matrices. The linear dispersion of Dirac fermions originates from the $d_{x^2-y^2}$ -wave symmetry of the energy gap of cuprate superconductor. Here, the spinor ψ_1^\dagger represents nodal quasiparticles excited from the $(\frac{\pi}{2}, \frac{\pi}{2})$ and $(-\frac{\pi}{2}, -\frac{\pi}{2})$ nodal points, and ψ_2^\dagger the other two nodal points [17]. The repeated spin index a is summed from 1 to N_f , the number of fermion spin components. The ratio $v_\Delta/v_F \approx 1/20$ between Fermi velocity and gap velocity is determined by experiments [25]. The effective action S_ϕ describes the Ising type nematic order parameter, which is expanded (for notational simplicity) in real space as

$$S_\phi = \int d^2\mathbf{x} d\tau \left\{ \frac{1}{2} (\partial\tau\phi)^2 + \frac{c^2}{2} (\nabla\phi)^2 + \frac{r}{2} \phi^2 + \frac{u_0}{24} \phi^4 \right\}, \quad (4)$$

where τ is imaginary time and c is velocity. The mass parameter r tunes the nematic phase transition with $r = 0$ defining the quantum critical point. The parameter u_0 is the quartic self-interaction strength. The nematic order parameter couples to nodal quasiparticles via the Yukawa term

$$S_{\psi\phi} = \int d^2\mathbf{x}d\tau \{ \lambda_0 \phi (\psi_{1a}^\dagger \tau^x \psi_{1a} + \psi_{2a}^\dagger \tau^x \psi_{2a}) \}. \quad (5)$$

Following Huh and Sachdev [19], we now perform the RG analysis in the framework of a $1/N_f$ expansion. The inverse of the free propagator of the nematic order parameter field behaves as $q^2 + r$. After taking into account the polarization effects, there will be an additional linear q -term. At low energy regime, the q -term dominates over the q^2 -term, which then can be neglected. Near the quantum critical point, we keep only the mass term and assume that $\phi \rightarrow \phi/\lambda_0$ and $r \rightarrow N_f r \lambda_0^2$, leading to

$$S = S_\psi + \int d^2\mathbf{x}d\tau \left\{ \frac{N_f r}{2} \phi^2 + \phi [\psi_{1a}^\dagger \tau^x \psi_{1a} + \psi_{2a}^\dagger \tau^x \psi_{2a}] \right\}. \quad (6)$$

After integrating out fermion degrees of freedom, the effective action for the scalar field becomes

$$\frac{S_\phi}{N} = \frac{1}{2} \int \frac{d^3q}{(2\pi)^3} [r + \Pi(q)] |\phi(q)|^2 + \mathcal{O}(\phi^4). \quad (7)$$

The lowest-order Feynman diagram for the polarization function is shown in Fig. 1 and symbolizes the integral

$$\Pi(\mathbf{q}, \epsilon) = \int \frac{d^2\mathbf{k}}{(2\pi)^2} \frac{d\omega}{2\pi} \text{Tr}[\tau^x G_\psi^0(\mathbf{k}, \omega) \tau^x G_\psi^0(\mathbf{k} + \mathbf{q}, \omega + \epsilon)],$$

where the free fermion propagator is

$$G_\psi^0(\mathbf{k}, \omega) = \frac{1}{-i\omega + v_F k_x \tau^z + v_\Delta k_y \tau^x}. \quad (8)$$

As shown previously [19], the propagator for the nematic order parameter is given by

$$\begin{aligned} G_\phi^{-1}(\mathbf{q}, \epsilon) &= \Pi(\mathbf{q}, \epsilon) \\ &= \frac{1}{16v_F v_\Delta} \frac{(\epsilon^2 + v_F^2 q_x^2)}{(\epsilon^2 + v_F^2 q_x^2 + v_\Delta^2 q_y^2)^{1/2}} \\ &\quad + \frac{1}{16v_F v_\Delta} \frac{(\epsilon^2 + v_F^2 q_y^2)}{(\epsilon^2 + v_F^2 q_x^2 + v_\Delta^2 q_y^2)^{1/2}} \end{aligned} \quad (9)$$

in the vicinity of nematic quantum critical point $r = 0$.

Disorders are present in almost all realistic condensed matter systems and play important roles in determining the low-temperature behaviors. In the present problem, the nodal quasiparticles can interact with three types of random potentials, which represent different disorder scattering processes. According to the coupling between nodal quasiparticle and disorders, there are three types of random fields in d -wave superconductors: random mass, random chemical potential, and random gauge potential. All these types of disorders have been investigated in the

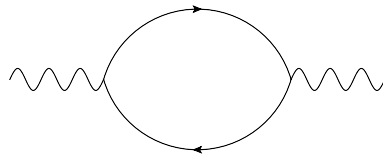


FIG. 1: The polarization function for nematic order parameter. The solid line represents the fermion propagator and wavy line represents the boson propagator.

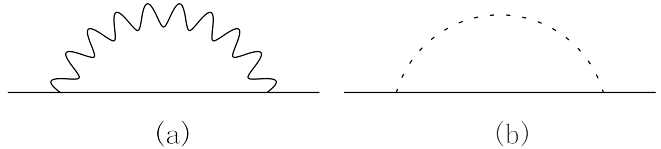


FIG. 2: One loop fermion self-energy correction due to (a) nematic order parameter fluctuation and (b) disorder. The dashed line represents disorder scattering.

contexts of d -wave cuprate superconductor [28, 29], quantum Hall effect [30], and graphene [31, 32]. In the general analysis to follow, we shall consider the three types of disorders.

The fermion field couples to a random field $A(\mathbf{x})$ as

$$\int d^2\mathbf{x} \psi^\dagger(\mathbf{x}) \Gamma \psi(\mathbf{x}) A(\mathbf{x}), \quad (10)$$

For random chemical potential, the matrix Γ is $\Gamma = \mathbb{I}$. For a random mass it is, $\Gamma = \tau^y$, and for a random gauge field $\Gamma = (\tau^x, \tau^z)$. The random potential $A(\mathbf{x})$ is assumed to be a quenched, Gaussian white noise field with the correlation functions

$$\langle A(\mathbf{x}) \rangle = 0; \quad \langle A(\mathbf{x}_1) A(\mathbf{x}_2) \rangle = g v_\Gamma^2 \delta^2(\mathbf{x}_1 - \mathbf{x}_2). \quad (11)$$

The dimensionless parameter g represents the concentration of impurity, and the parameter v_Γ measures the strength of a single impurity. It will be convenient to redefine the random potential as $A(\mathbf{x}) \rightarrow v_\Gamma A(\mathbf{x})$, and then write the fermion-disorder interaction term as [31]

$$S_{\text{dis}} = v_\Gamma \int d^2\mathbf{x} \psi^\dagger(\mathbf{x}) \Gamma \psi(\mathbf{x}) A(\mathbf{x}), \quad (12)$$

with the random potential distribution

$$\langle A(\mathbf{x}) \rangle = 0; \quad \langle A(\mathbf{x}_1) A(\mathbf{x}_2) \rangle = g \delta^2(\mathbf{x}_1 - \mathbf{x}_2). \quad (13)$$

Now the RG flow of disorder strength can be calculated by studying the vertex correction to the fermion-disorder interaction term. After a Fourier transformation, the corresponding action has the form

$$S_{\text{dis}} = v_\Gamma \int d^2\mathbf{k} d^2\mathbf{k}_1 d\omega \psi^\dagger(\mathbf{k}, \omega) \Gamma \psi(\mathbf{k}_1, \omega) A(\mathbf{k} - \mathbf{k}_1). \quad (14)$$

This action will be analyzed together with the actions (3), (6), and (7). In order to perform perturbative expansion, we assume that g and v_Γ are both small in magnitude, corresponding to the weak disorder case.

III. FERMION SELF-ENERGY AND FERMION-DISORDER VERTEX CORRECTIONS

According to the Dyson equation, the interactions induce a self-energy correction to the free propagator of Dirac fermion, yielding

$$G_{\psi}^{-1}(\mathbf{k}, \omega) = -i\omega + v_F k_x \tau^z + v_{\Delta} k_y \tau^x - \Sigma_{\text{nm}}(\mathbf{k}, \omega) - \Sigma_{\text{dis}}(\mathbf{k}, \omega), \quad (15)$$

where self-energy functions Σ_{nm} and Σ_{dis} come from nematic ordering and disorder scattering, respectively. To the leading order, the corresponding Feynman diagrams are presented in Fig. 2.

The nematic self-energy Σ_{nm} has already been obtained by Huh and Sachdev [19], who found that

$$\frac{d\Sigma_{\text{nm}}(\mathbf{k}, \omega)}{d \ln \Lambda} = C_1(-i\omega) + C_2 v_F k_x \tau^z + C_3 v_{\Delta} k_y \tau^x, \quad (16)$$

where

$$C_1 = \frac{2(v_{\Delta}/v_F)}{N_f \pi^3} \int_{-\infty}^{\infty} dx \int_0^{2\pi} d\theta \times \frac{x^2 - \cos^2 \theta - (v_{\Delta}/v_F)^2 \sin^2 \theta}{(x^2 + \cos^2 \theta + (v_{\Delta}/v_F)^2 \sin^2 \theta)^2} \mathcal{G}(x, \theta), \quad (17)$$

$$C_2 = \frac{2(v_{\Delta}/v_F)}{N_f \pi^3} \int_{-\infty}^{\infty} dx \int_0^{2\pi} d\theta \times \frac{\cos^2 \theta - x^2 - (v_{\Delta}/v_F)^2 \sin^2 \theta}{(x^2 + \cos^2 \theta + (v_{\Delta}/v_F)^2 \sin^2 \theta)^2} \mathcal{G}(x, \theta), \quad (18)$$

$$C_3 = \frac{2(v_{\Delta}/v_F)}{N_f \pi^3} \int_{-\infty}^{\infty} dx \int_0^{2\pi} d\theta \times \frac{x^2 + \cos^2 \theta - (v_{\Delta}/v_F)^2 \sin^2 \theta}{(x^2 + \cos^2 \theta + (v_{\Delta}/v_F)^2 \sin^2 \theta)^2} \mathcal{G}(x, \theta), \quad (19)$$

$$\mathcal{G}^{-1} = \frac{x^2 + \cos^2 \theta}{\sqrt{x^2 + \cos^2 \theta + (v_{\Delta}/v_F)^2 \sin^2 \theta}} + \frac{x^2 + \sin^2 \theta}{\sqrt{x^2 + \sin^2 \theta + (v_{\Delta}/v_F)^2 \cos^2 \theta}}. \quad (20)$$

The computational details of $C_{1,2,3}$ are presented in the appendix.

The fermion self-energy due to disorder $\Sigma_{\text{dis}}(i\omega)$ can be computed as

$$\begin{aligned} \Sigma_{\text{dis}}(i\omega) &= g v_{\Gamma}^2 \int \frac{d^2 \mathbf{k}}{(2\pi)^2} \Gamma G_{\psi}^0(\mathbf{k}, \omega) \Gamma \\ &= \frac{g v_{\Gamma}^2}{2\pi v_F v_{\Delta}} i\omega \ln \Lambda. \end{aligned} \quad (21)$$

From this expression, we know that $\Sigma_{\text{dis}}(i\omega)$ has the same result for all possible expressions of Γ . Another important feature is that $\Sigma_{\text{dis}}(i\omega)$ is independent of momentum, which reflects the fact that the quenched disorder is static. It is easy to have

$$\frac{d\Sigma_{\text{dis}}(i\omega)}{d \ln \Lambda} = C_g i\omega, \quad (22)$$

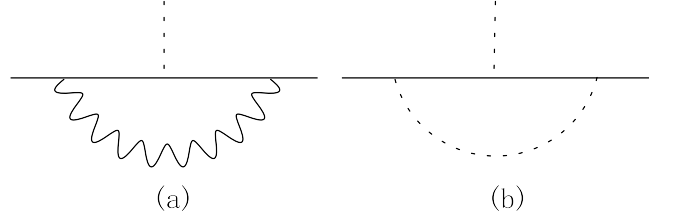


FIG. 3: Fermion-disorder vertex correction due to (a) nematic order parameter and (b) disorder parameter.

where

$$C_g = \frac{g v_{\Gamma}^2}{2\pi v_F v_{\Delta}}. \quad (23)$$

The fermion-disorder interaction parameter v_{Γ} is also subjected to RG flow. To get its flow equation, we need to calculate the fermion-disorder vertex corrections. Formally, the vertex correction has the form

$$v_{\Gamma} \Gamma' = v_{\Gamma} \Gamma + V_{\text{nm}} + V_{\text{dis}}, \quad (24)$$

where V_{nm} represents the vertex correction due to nematic order parameter fluctuation and V_{dis} represents the vertex correction due to disorder interaction. The corresponding diagrams are shown in Fig. 3. They will be calculated explicitly in the following for all three kinds of disorders.

1. Random chemical potential

We first calculate the vertex correction due to nematic ordering. To this end, we employ the method proposed by Huh and Sachdev [19]. At zero external momenta and frequencies, the vertex correction is expressed as

$$V_{\text{nm}} = v_{\Gamma} \int \frac{d^3 Q}{(2\pi)^3} H(Q) \mathcal{K}^3\left(\frac{\mathbf{q}^2}{\Lambda^2}\right). \quad (25)$$

There is an useful formula [19],

$$\frac{dV_{\text{nm}}}{d \ln \Lambda} = v_{\Gamma} \frac{v_F}{8\pi^3} \int_{-\infty}^{\infty} dx \int_0^{2\pi} d\theta H(\hat{Q}), \quad (26)$$

where

$$\begin{aligned} H(\hat{Q}) &= \frac{1}{N_f} \tau^x \frac{1}{(-iv_F x + v_F \cos \theta \tau^z + v_{\Delta} \sin \theta \tau^x)} \mathbf{I} \\ &\times \frac{1}{(-iv_F x + v_F \cos \theta \tau^z + v_{\Delta} \sin \theta \tau^x)} \tau^x \frac{1}{\Pi(\hat{Q})}. \end{aligned} \quad (27)$$

Here, the matrix \mathbf{I} corresponds to the coupling between Dirac fermion and random chemical potential. It will be replaced by τ^y in the case of random mass and $\tau^{x,z}$ in

the case of random gauge field. After straightforward computation, we have

$$\frac{dV_{\text{nm}}}{d \ln \Lambda} = C_5 v_\Gamma \mathbf{I}, \quad (28)$$

where

$$\begin{aligned} C_5 &= -\frac{2(v_\Delta/v_F)}{N_f \pi^3} \int_{-\infty}^{\infty} dx \int_0^{2\pi} d\theta \\ &\quad \times \frac{(x^2 - \cos^2 \theta - (v_\Delta/v_F)^2 \sin^2 \theta)}{(x^2 + \cos^2 \theta + (v_\Delta/v_F)^2 \sin^2 \theta)^2} \mathcal{G}(x, \theta) \\ &= -C_1. \end{aligned} \quad (29)$$

The vertex correction due to averaging over disorder is

$$V_{\text{dis}} = g v_\Gamma^2 \int \frac{d^2 \mathbf{p}}{(2\pi)^2} \text{IG}_\psi^0(\omega, \mathbf{p}) v_\Gamma \text{IG}_\psi^0(\omega, \mathbf{p} + \mathbf{k}) \mathbf{I}. \quad (30)$$

Again, the matrix \mathbf{I} should be replaced by certain Pauli matrix in the case of random mass or random gauge field. Taking the external momentum $\mathbf{k} = 0$ and keeping only the leading divergent term, we have

$$\frac{dV_{\text{dis}}}{d \ln \Lambda} = C_\Gamma v_\Gamma \mathbf{I}, \quad (31)$$

where

$$C_\Gamma = \frac{v_\Gamma^2 g}{2\pi v_F v_\Delta} = C_g. \quad (32)$$

2. Random mass

The calculation of vertex correction in the case of random mass parallels the process presented above, so we just state the final result. The nematic ordering induced vertex correction is

$$\frac{dV_{\text{nm}}}{d \ln \Lambda} = C_6 v_\Gamma \tau^y, \quad (33)$$

where

$$\begin{aligned} C_6 &= \frac{2(v_\Delta/v_F)}{N_f \pi^3} \int_{-\infty}^{\infty} dx \int_0^{2\pi} d\theta \\ &\quad \times \frac{(x^2 + \cos^2 \theta + (v_\Delta/v_F)^2 \sin^2 \theta)}{(x^2 + \cos^2 \theta + (v_\Delta/v_F)^2 \sin^2 \theta)^2} \mathcal{G}(x, \theta) \\ &= C_3 - C_1 - C_2. \end{aligned} \quad (34)$$

The disorder induced vertex correction is

$$\frac{dV_{\text{dis}}}{d \ln \Lambda} = -C_\Gamma (v_\Gamma \tau^y), \quad (35)$$

where

$$C_\Gamma = \frac{v_\Gamma^2 g}{2\pi v_F v_\Delta} = C_g. \quad (36)$$

3. Random gauge potential

The random gauge potential has two components, characterized by τ^x and τ^z respectively. For the τ^x component, the nematic ordering contribution to vertex correction is

$$\frac{dV_{\text{nm}}}{d \ln \Lambda} = C_{4A} v_\Gamma \tau^x, \quad (37)$$

where

$$\begin{aligned} C_{4A} &= -\frac{2(v_\Delta/v_F)}{N_f \pi^3} \int_{-\infty}^{\infty} dx \int_0^{2\pi} d\theta \\ &\quad \times \frac{(x^2 + \cos^2 \theta - (v_\Delta/v_F)^2 \sin^2 \theta)}{(x^2 + \cos^2 \theta + (v_\Delta/v_F)^2 \sin^2 \theta)^2} \mathcal{G}(x, \theta) \\ &= -C_3. \end{aligned} \quad (38)$$

For the τ_z component, we have

$$\frac{dV_{\text{nm}}}{d \ln \Lambda} = C_{4B} v_\Gamma \tau^z, \quad (39)$$

where

$$\begin{aligned} C_{4B} &= -\frac{2(v_\Delta/v_F)}{N_f \pi^3} \int_{-\infty}^{\infty} dx \int_0^{2\pi} d\theta \\ &\quad \times \frac{(x^2 - \cos^2 \theta + (v_\Delta/v_F)^2 \sin^2 \theta)}{(x^2 + \cos^2 \theta + (v_\Delta/v_F)^2 \sin^2 \theta)^2} \mathcal{G}(x, \theta) \\ &= -C_2. \end{aligned} \quad (40)$$

The disorder contribution can be calculated similarly. To both the τ^x and τ^z component, we have

$$V_{\text{dis}}(\omega) = \text{finite}, \quad (41)$$

so that

$$\frac{dV_{\text{dis}}}{d \ln \Lambda} = 0. \quad (42)$$

for both two components.

IV. RG EQUATIONS FOR FERMION VELOCITIES AND DISORDER STRENGTH

In order to perform the RG analysis of the fermion velocity and disorder strength, it is convenient to make the following scaling transformations [19, 33]

$$k_i = k'_i e^{-l}, \quad (43)$$

$$\omega = \omega' e^{-l}, \quad (44)$$

$$\psi_{1,2}(\mathbf{k}, \omega) = \psi'_{1,2}(\mathbf{k}', \omega') e^{\frac{1}{2} \int_0^l (4 - \eta_f) dl}, \quad (45)$$

$$\phi(\mathbf{q}, \epsilon) = \phi'(\mathbf{q}', \epsilon') e^{\frac{1}{2} \int_0^l (5 - \eta_b) dl}, \quad (46)$$

where $i = x, y$ and $b = e^{-l}$ with $l > 0$. The parameters η_f and η_b will be determined by the self-energy and nematic-fermion vertex corrections. Note the energy is required to

scale in the same way as the momentum, so the fermion velocities are forced to flow under RG transformations.

In the spirit of RG theory [33], to specify how a field operator transforms when the energy and momenta are re-scaled, the standard method is to require that its kinetic term remains invariant. In the present problem, however, the random potential $A(\mathbf{x})$ does not have an own kinetic term. In order to find out its scaling behavior, we write the Gaussian white noise distribution in the momentum space as

$$\langle A(\mathbf{k}_1)A(\mathbf{k}_2) \rangle = g\delta^2(\mathbf{k}_1 + \mathbf{k}_2). \quad (47)$$

When the momentum \mathbf{k} becomes $b\mathbf{k}$, the delta function is rescaled to

$$\delta^2(\mathbf{k}_1 + \mathbf{k}_2) \rightarrow \delta^2(b\mathbf{k}_1 + b\mathbf{k}_2) = b^{-2}\delta^2(\mathbf{k}_1 + \mathbf{k}_2). \quad (48)$$

If we require that the disorder distribution Eq. (47) is invariant under scaling transformations, then the random potential should transform as

$$A(\mathbf{k}) \rightarrow b^{-1}A(\mathbf{k}). \quad (49)$$

Now we have to assume that

$$A(\mathbf{k}) = A'(\mathbf{k}')e^l. \quad (50)$$

According to the RG technique presented in [33], the momentum shell between $b\Lambda$ and Λ will be integrated out, while keeping the $-i\omega$ term invariant. From the nematic ordering and disorder contributions to fermion self-energy function, we have

$$\begin{aligned} & \int^{b\Lambda} d^2\mathbf{k}d\omega\psi^\dagger[-i\omega - C_1(-i\omega)\ln\frac{\Lambda}{b\Lambda} + C_g(-i\omega)\ln\frac{\Lambda}{b\Lambda}]\psi \\ &= \int^{b\Lambda} d^2\mathbf{k}d\omega\psi^\dagger(-i\omega)[1 + (C_g - C_1)l]\psi \\ &\approx \int^{b\Lambda} d^2\mathbf{k}d\omega\psi^\dagger(-i\omega)e^{(C_g - C_1)l}\psi. \end{aligned} \quad (51)$$

After the scaling transformation, this term should go back to the free form, so that

$$\eta_f = C_g - C_1. \quad (52)$$

The kinetic terms should also be kept invariant under scaling transformation, which leads to

$$\frac{dv_F}{dl} = (C_1 - C_2 - C_g)v_F, \quad (53)$$

$$\frac{dv_\Delta}{dl} = (C_1 - C_3 - C_g)v_\Delta. \quad (54)$$

Based on these expressions, the ratio between gap velocity and Fermi velocity is

$$\frac{d(v_\Delta/v_F)}{dl} = (C_2 - C_3)(v_\Delta/v_F). \quad (55)$$

The disorder strength g appears in the above expressions. Due to the interplay of nematic ordering and disorder, this parameter also flows under RG transformation. The flow equation depends on the type of disorder, which will be studied in the following.

We first consider the case of random chemical potential. The bare fermion-disorder action is

$$v_\Gamma \int d^2\mathbf{k}d^2\mathbf{k}_1d\omega\psi^\dagger(\mathbf{k}, \omega)\Gamma\psi(\mathbf{k}_1, \omega)A(\mathbf{k} - \mathbf{k}_1). \quad (56)$$

Including corrections due to nematic and disorder interactions yields

$$\begin{aligned} & \int^{b\Lambda} d^2\mathbf{k}d^2\mathbf{k}_1d\omega\psi^\dagger(\mathbf{k}, \omega)[v_\Gamma\mathbb{I} - C_1v_\Gamma\mathbb{I}\ln\frac{\Lambda}{b\Lambda} \\ & + C_gv_\Gamma\mathbb{I}\ln\frac{\Lambda}{b\Lambda}]\psi(\mathbf{k}_1, \omega)A(\mathbf{k} - \mathbf{k}_1) \\ &= \int^{b\Lambda} d^2\mathbf{k}d^2\mathbf{k}_1d\omega\psi^\dagger(\mathbf{k}, \omega)v_\Gamma\mathbb{I}[1 + (C_g - C_1)l] \\ & \times \psi(\mathbf{k}_1, \omega)A(\mathbf{k} - \mathbf{k}_1) \\ &\approx \int^{b\Lambda} d^2\mathbf{k}d^2\mathbf{k}_1d\omega\psi^\dagger(\mathbf{k}, \omega)v_\Gamma\mathbb{I}e^{(C_g - C_1)l} \\ & \times \psi(\mathbf{k}_1, \omega)A(\mathbf{k} - \mathbf{k}_1). \end{aligned} \quad (57)$$

After redefining energy, momentum, and field operators, we have

$$\begin{aligned} & \int^\Lambda d^2\mathbf{k}'d^2\mathbf{k}'_1d\omega'\psi'^\dagger(\mathbf{k}', \omega')v_\Gamma\mathbb{I} \\ & \times e^{(C_g - C_1)l}\psi'(\mathbf{k}'_1, \omega')e^{-\eta_f l}A'(\mathbf{k}' - \mathbf{k}'_1). \end{aligned} \quad (58)$$

Since $\eta_f = C_g - C_1$, it is easy to obtain the following RG flow equation for v_Γ ,

$$\frac{dv_\Gamma}{dl} = 0. \quad (59)$$

Apparently, the parameter v_Γ does not flow and thus can be simply taken to be a constant.

In the case of random mass, the flow equations for fermion velocities have the same expressions as Eq.(53) and Eq.(54). However, the flow equation for disorder strength is different from Eq.(58), and has the form

$$\frac{dv_\Gamma}{dl} = (C_3 - C_2 - 2C_g)v_\Gamma, \quad (60)$$

which couples self-consistently to flow equations of fermion velocities.

Following the steps presented above, we find the following RG equations in the case of random gauge potential

$$\frac{dv_F}{dl} = (C_1 - C_2 - C_{gi})v_F, \quad (61)$$

$$\frac{dv_\Delta}{dl} = (C_1 - C_3 - C_{gi})v_\Delta, \quad (62)$$

which couple to the flow equations of disorder strength

$$\frac{dv_{\Gamma 1}}{dl} = [(C_1 - C_{g1}) - C_3]v_{\Gamma 1}, \quad (63)$$

$$\frac{dv_{\Gamma 2}}{dl} = [(C_1 - C_{g2}) - C_2]v_{\Gamma 2}, \quad (64)$$

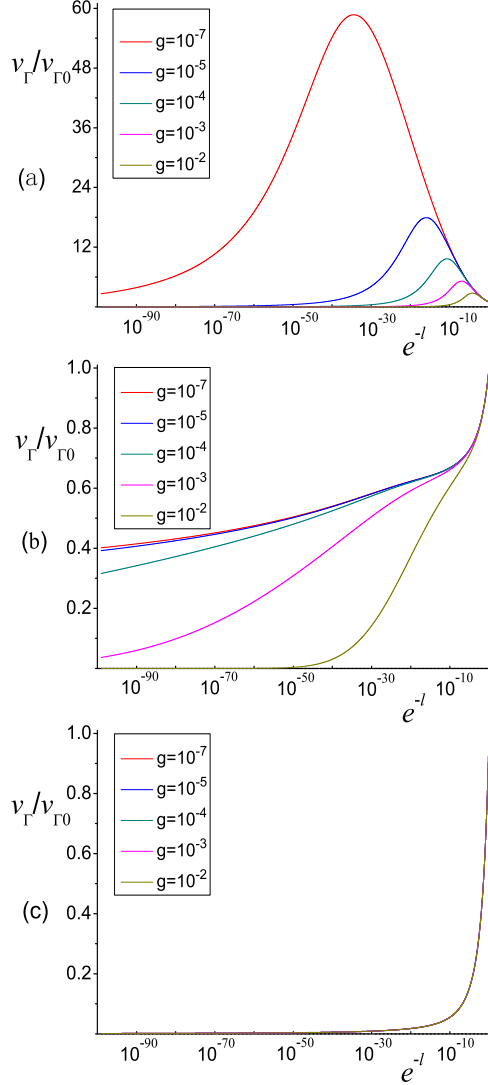


FIG. 4: (a) v_Γ for random mass; (b) v_Γ for random gauge potential τ^x component; (c) v_Γ for random gauge potential τ^z component.

where

$$C_{g_i} = \frac{v_{\Gamma i}^2 g}{2\pi v_F v_\Delta}, \quad i = 1, 2. \quad (65)$$

Here, the equations denoted by $i = 1, 2$ correspond to the τ^x and τ^z components of random gauge potential, respectively.

V. STABILITY OF EXTREME ANISOTROPY AGAINST DISORDERS

The RG flows of fermion velocities v_F and v_Δ with growing scale l can be obtained by numerically solving the corresponding coupled equations with the initial values v_{F0} , $v_{\Delta 0}$, and $v_{\Gamma 0}$. First of all, in the clean limit

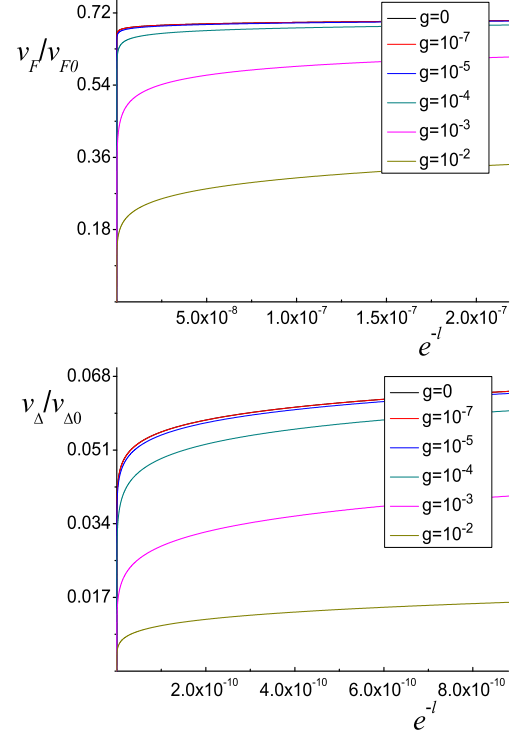


FIG. 5: The flows of v_F (upper one) and v_Δ (lower one) in the case of random mass.

$g = 0$, the equations reduce to that obtained by Huh and Sachdev. In this case, it was already known that an extreme anisotropy of fermion velocities, i.e., $v_\Delta/v_F \rightarrow 0$, is caused by nematic order parameter fluctuation. The effects of various disorders on this fixed point will be transparent when the dimensionless parameter g is increased smoothly.

We first consider the case of random mass. As l grows, v_Γ first increases and then decreases, eventually approaching zero, as shown in Fig. 4(a). Although the RG equations for fermion velocities are modified by scattering due to random mass, the disorder parameter v_Γ flows to zero as $l \rightarrow \infty$. Apparently, the random mass is irrelevant in the present problem. As can be easily seen from see Fig. 5, the fermion velocities v_F and v_Δ both decrease as l grows. More concretely, v_Δ goes down to zero rapidly, but v_F decreases much more slowly and actually approaches a finite value. These results imply the existence of extreme velocity anisotropy with $v_\Delta/v_F \rightarrow 0$ in the presence of random mass.

We next discuss the case of random gauge potential. The flows of disorder strength v_Γ with growing l are shown in Fig. 4(b) for component τ^x and in Fig. 4(c) for component τ^z . For both components, the corresponding v_Γ decrease as l grows and finally approaches zero as $l \rightarrow \infty$. Similar to the case of random mass, the random gauge potential makes no important contributions to the flow of fermion velocities. Therefore, as in the clean limit, both v_F and v_Δ decreases with l until approaching zero

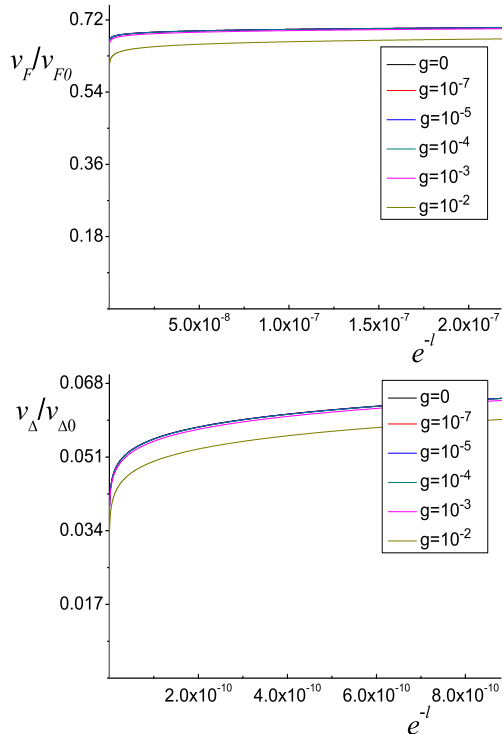


FIG. 6: The running v_F and v_Δ for the τ^x component of random gauge potential. The running of fermion velocities for component τ^z are very similar to this case, and thus are not shown.

for component τ^x depicted in Fig. 6; the flows of v_F and v_Δ for component τ^z with growing l will not be shown since they are similar to those in the case of component τ^x . It is obvious that random gauge potential does not change the extreme velocity anisotropy.

Unlike random mass and random gauge potential, the disorder strength parameter v_Γ in the case of random chemical potential does not flow with l and thus should be kept as a constant. As such, the influence of scattering due to random chemical potential can not be neglected and indeed the flows of velocities v_F and v_Δ depend heavily on the magnitude of v_Γ . At first glance, the flow equation of velocity ratio v_Δ/v_F is independent of disorder strength v_Γ , as shown in Eq. (55), and thus appears to have fixed point at $v_\Delta/v_F = 0$ as in the clean limit. However, this solution is artificial. In the present problem, the flow equation of v_Δ/v_F is derived from the more fundamental equations of v_Δ and v_F , and therefore is reliable only when v_Δ and v_F have well-defined fixed points. If the equations for v_Δ and v_F have no fixed points, the equation of v_Δ/v_F becomes meaningless.

To see the effect of random chemical potential, we make a qualitative analysis based on the RG equations of fermion velocities v_Δ and v_F . The fixed points can be obtained by requiring that

$$\frac{dv_F}{dl} = (C_1 - C_2)v_F - \frac{v_\Gamma^2 g}{2\pi v_\Delta} = 0, \quad (66)$$

$$\frac{dv_\Delta}{dl} = (C_1 - C_3)v_\Delta - \frac{v_\Gamma^2 g}{2\pi v_F} = 0. \quad (67)$$

We assume that v_F^* and v_Δ^* correspond to the fixed points. If both v_F^* and v_Δ^* are finite, then the above equations imply that $(C_1 - C_2)v_\Delta^* v_F^* = (C_1 - C_3)v_\Delta^* v_F^*$, which can not be satisfied since $v_\Delta^* \neq 0$. If $v_\Delta^* = 0$, then

$$v_F^* = \frac{v_\Gamma^2 g}{2\pi v_\Delta^* (C_1 - C_2)}. \quad (68)$$

From the expressions for C_1 and C_2 , this implies that $1 \propto 1/(v_\Delta^*)^2$, which is clearly inconsistent with the assumption of $v_\Delta^* = 0$. Before going to $v_F^* = 0$ case, we define $D_i = (v_F/v_\Delta)C_i, i = (1, 2, 3)$, then the new forms of Eq.(66) and Eq.(67) become

$$(D_1 - D_2)v_\Delta = \frac{v_\Gamma^2 g}{2\pi v_\Delta}, \quad (69)$$

$$(D_1 - D_3)\frac{v_\Delta}{v_F} = \frac{v_\Gamma^2 g}{2\pi v_F}. \quad (70)$$

If $v_F^* = 0$, by both analytical and numerical analysis, we found that these equations have no solution.

In summary, as shown by the above analysis, there is no fixed point of the fermion velocities v_F and v_Δ when the fermions interact with random chemical potential. Therefore, v_F and v_Δ do not approach any stable values at the low energy regime. Alternatively, straightforward numerical calculations show that they oscillate rapidly between positive and unphysical negative values as l grows. In this case, the extreme velocity anisotropy fixed point is destroyed. We interpret the occurrence of unphysical negative velocities as a signature of the instability of nematic phase transition in the presence of random chemical potential.

VI. SUMMARY AND DISCUSSION

In summary, we have examined the disorder effect near the critical point of nematic phase transition in d -wave cuprate superconductor. We considered three types of quenched disorders that couple directly to the gapless nodal quasiparticles: random mass, random gauge field, and random chemical potential. By means of a RG analysis, we have derived a series of self-consistent flow equations for fermion velocities and disorder strength. It was found that the fixed point of extreme velocity anisotropy due to critical fluctuation of nematic order parameter is not changed by random mass and random gauge field, which are both irrelevant at low energy. Therefore, it seems reasonable to expect an enhancement of dc thermal conductivity at low temperature if there are only these two kinds of disorders. However, when there is moderately strong random chemical potential, which is marginal, the extreme anisotropy fixed point is destroyed. Moreover, the nematic phase transition may become unstable in the presence of such random chemical potential.

The extreme velocity anisotropy produced by the critical nematic fluctuations may be probed by the heat transport measurements, since it leads to a remarkable enhancement of the low-temperature thermal conductivity. Apart from transport measurements, such extreme anisotropy can also show its existence in angle-resolved photo-emission spectroscopy (ARPES) experiments. Indeed, the currently known value of the velocity ratio v_Δ/v_F in d -wave cuprate superconductors was extracted from both heat transport [34] and ARPES measurements [35]. Unlike heat transport experiments that can only estimate the ratio v_Δ/v_F , the ARPES measurements are able to determine the Fermi velocity v_F and the gap velocity v_Δ separately [35]. From the solutions of RG equations, we know that, the extreme velocity anisotropy emerges because v_Δ is driven by the critical nematic fluctuations to drop rapidly down to zero at large l but v_F is driven to decrease very slowly. It should be possible to detect the extreme anisotropy by measuring v_F and v_Δ separately by means of the ARPES experiments.

In addition, the effects of the nematic order parameter fluctuations can also be reflected in the single-particle spectral function of nodal quasiparticles. Kim *et al.* [18] investigated this issue and found two important features: strong angle-dependence of quasiparticle scattering, and an enhancement of velocity anisotropy. These predicted features of the fermion spectral function are expected to be tested by ARPES experiments.

We next would like to remark on the disorder effects on the polarization function and the final results. In our calculations, the polarization function is obtained from the bubble diagram shown in Fig. 1, since including internal disorder scattering line will introduce an additional suppressing factor $g v_F^2$. To justify this approximation, we now make a qualitative analysis on the disorder effects. It is well known that disorder scattering generates a fermion damping rate γ_0 , which shifts the energy of Dirac fermions from ω to $\omega + i\gamma_0$. In the presence of finite γ_0 , it seems possible to get a full analytical expression for the polarization function $\Pi(q_x, q_y, \epsilon)$ only in the static ($\epsilon = 0$) limit. Following the computational procedures given in [36, 37], we have

$$\begin{aligned} \Pi(q_x, q_y, \gamma_0) &= \frac{1}{2\pi^2 v_F v_\Delta} \int_0^1 dx \frac{2\sqrt{x(1-x)} v_F^2 q_x^2}{\sqrt{v_F^2 q_x^2 + v_\Delta^2 q_y^2}} \\ &\times \arctan\left(\gamma_0^{-1} \sqrt{x(1-x)}(v_F^2 q_x^2 + v_\Delta^2 q_y^2)\right) \\ &+(q_x \longleftrightarrow q_y). \end{aligned} \quad (71)$$

In order to simplify this expression, we now consider the low-energy regime, $|\mathbf{q}| \leq \gamma_0$, which leads to $\arctan\left(\gamma_0^{-1} \sqrt{x(1-x)}(v_F^2 q_x^2 + v_\Delta^2 q_y^2)\right) \approx \gamma_0^{-1} \sqrt{x(1-x)}(v_F^2 q_x^2 + v_\Delta^2 q_y^2)$. Using this approximation, the polarization function is found to be

$$\Pi(q_x, q_y, \gamma_0) = \frac{v_F}{6\pi^2 v_\Delta \gamma_0} (q_x^2 + q_y^2). \quad (72)$$

Substituting this new polarization to the nematic propagator and then performing the same RG calculations, we found that the qualitative results presented in Sec. V do not change. We thus conclude that it is justified to neglect disorder effects in the polarization function for weak disorders. Admittedly, when disorders are strong enough to cause Anderson localization, the RG approach utilized in our manuscript is no longer applicable and a new RG scheme is needed to deal with the vertex corrections generated by disorder scattering.

In this paper, we have considered only the coupling between disorders and fermionic nodal quasiparticles since we are mainly interested in the disorder effects on the RG flow of fermion velocities. In practice, the effects of disorders on the nematic transition are more complicated. For instance, there might be quenched disorders that couple directly to the nematic order parameter. This issue was briefly discussed by Kim *et al.*, who argued [18] that quenched disorder may smear the symmetry-breaking type quantum phase transition thereby producing a glassy state. It is currently unclear how the nodal quasiparticles are influenced by such kind of disorders.

VII. ACKNOWLEDGMENTS

G.Z.L. and H.K. would like to thank Flavio S. Nogueira for valuable discussions. J.W. is grateful to Wei Li and Jing-Rong Wang for their helps. G.Z.L. acknowledges the financial support from the National Science Foundation of China under Grant No.11074234 and the project sponsored by the Overseas Academic Training Funds of University of Science and Technology of China.

Appendix

In order to maintain a self-consistency of this paper, here we provide a detailed calculation of the fermion self-energy (16). Following Ref. [19], we can define

$$\Sigma_{\text{nm}}(K) = \int \frac{d^3 Q}{(2\pi)^3} F(Q+K) G(Q) \mathcal{K}\left(\frac{(\mathbf{q}+\mathbf{k})^2}{\Lambda^2}\right) \mathcal{K}\left(\frac{\mathbf{q}^2}{\Lambda^2}\right), \quad (73)$$

where $K \equiv (\mathbf{k}, \omega)$ and $Q \equiv (\mathbf{q}, \epsilon)$ are 3-momenta. Here $\mathcal{K}(y)$ is an arbitrary function with $\mathcal{K}(0) = 1$, and it falls off rapidly with y , e.g. $\mathcal{K}(y) = e^{-y}$. However, the results are independent of the particular choices of $\mathcal{K}(y)$. It is easy to

identify that,

$$G(Q) = \frac{1}{\Pi(\mathbf{q}, \epsilon)}, \quad (74)$$

$$F(Q + K) = \frac{1}{N_f} \frac{i(\epsilon + \omega) - v_F(q_x + k_x)\tau^z + v_\Delta(q_y + k_y)\tau^x}{(\epsilon + \omega)^2 + v_F^2(q_x + k_x)^2 + v_\Delta^2(q_y + k_y)^2}. \quad (75)$$

Expanding $F(Q + K)\mathcal{K}\left(\frac{(\mathbf{q} + \mathbf{k})^2}{\Lambda^2}\right)$ at $Q + K = Q$, and retaining the first order, we have

$$\begin{aligned} & F(Q + K)\mathcal{K}\left(\frac{(\mathbf{q} + \mathbf{k})^2}{\Lambda^2}\right) \\ & \approx K_\mu \left[\frac{\partial F(Q + K)}{\partial Q_\mu} \mathcal{K}\left(\frac{(\mathbf{q} + \mathbf{k})^2}{\Lambda^2}\right) + F(Q + K) \frac{2(\mathbf{q} + \mathbf{k})_\mu}{\Lambda^2} \mathcal{K}'\left(\frac{(\mathbf{q} + \mathbf{k})^2}{\Lambda^2}\right) \right] \Big|_{Q_\mu + K_\mu = Q_\mu} \\ & = K_\mu \left[\frac{\partial F(Q)}{\partial Q_\mu} \mathcal{K}\left(\frac{\mathbf{q}^2}{\Lambda^2}\right) + F(Q) \frac{2q_\mu}{\Lambda^2} \mathcal{K}'\left(\frac{\mathbf{q}^2}{\Lambda^2}\right) \right]. \end{aligned} \quad (76)$$

Then the self-energy becomes

$$\Sigma_{\text{nm}}(K) \approx K_\mu \int \frac{d^3Q}{(2\pi)^3} \left[\frac{\partial F(Q)}{\partial Q_\mu} G(Q) \mathcal{K}^2\left(\frac{\mathbf{q}^2}{\Lambda^2}\right) + F(Q) G(Q) \frac{2q_\mu}{\Lambda^2} \mathcal{K}\left(\frac{\mathbf{q}^2}{\Lambda^2}\right) \mathcal{K}'\left(\frac{\mathbf{q}^2}{\Lambda^2}\right) \right], \quad (77)$$

which leads to

$$\begin{aligned} \frac{d\Sigma_{\text{nm}}(K)}{d\Lambda} &= K_\mu \int \frac{d^3Q}{(2\pi)^3} \left\{ \left[\frac{-4\mathbf{q}^2}{\Lambda^2} \frac{\partial F(Q)}{\partial Q_\mu} - 4F(Q) \frac{q_\mu}{\Lambda^2} \right] G(Q) \mathcal{K}\left(\frac{\mathbf{q}^2}{\Lambda^2}\right) \mathcal{K}'\left(\frac{\mathbf{q}^2}{\Lambda^2}\right) \right. \\ & \quad \left. - \frac{4\mathbf{q}^2 q_\mu}{\Lambda^4} F(Q) G(Q) \left[\mathcal{K}\left(\frac{\mathbf{q}^2}{\Lambda^2}\right) \mathcal{K}''\left(\frac{\mathbf{q}^2}{\Lambda^2}\right) + \mathcal{K}'^2\left(\frac{\mathbf{q}^2}{\Lambda^2}\right) \right] \right\}. \end{aligned} \quad (78)$$

It is convenient to introduce the following cylindrical coordinates,

$$\begin{aligned} Q_\mu &= y\Lambda(v_F x, \cos\theta, \sin\theta), \\ \hat{Q}_\mu &= (v_F x, \cos\theta, \sin\theta), \\ q_\mu &= y\Lambda(0, \cos\theta, \sin\theta), \\ \hat{q}_\mu &= (0, \cos\theta, \sin\theta), \\ d^3Q &= y^2 \Lambda^3 v_F dx dy d\theta. \end{aligned}$$

It is straightforward to obtain

$$\begin{aligned} F(\hat{Q}) &= \frac{1}{N_f v_F} \left(\frac{ix - \cos\theta\tau^z + (v_\Delta/v_F)\sin\theta\tau^x}{x^2 + \cos^2\theta + (v_\Delta/v_F)^2 \sin^2\theta} \right), \\ G(\hat{Q}) &= \frac{1}{\Pi(\hat{Q})} = 16v_\Delta \mathcal{G}(x, \theta), \end{aligned} \quad (79)$$

where

$$\begin{aligned} \mathcal{G}^{-1} &= \frac{x^2 + \cos^2\theta}{\sqrt{x^2 + \cos^2\theta + (v_\Delta/v_F)^2 \sin^2\theta}} \\ & \quad + \frac{x^2 + \sin^2\theta}{\sqrt{x^2 + \sin^2\theta + (v_\Delta/v_F)^2 \cos^2\theta}}. \end{aligned} \quad (80)$$

Since F and G are homogenous functions,

$$F(Q) = \frac{1}{y\Lambda} F(\hat{Q}), \quad G(Q) = \frac{1}{y\Lambda} G(\hat{Q}). \quad (81)$$

We thus have

$$\begin{aligned}
\Lambda \frac{d\Sigma_{\text{nm}}(K)}{d\Lambda} &\approx \frac{v_F K_\mu}{(2\pi)^3} \int_{-\infty}^{\infty} dx \int_0^{2\pi} d\theta \int_0^{\infty} dy \left\{ \left[-4y \frac{\partial F(\hat{Q})}{\partial \hat{Q}_\mu} - 4y \hat{q}_\mu F(\hat{Q}) \right] G(\hat{Q}) \mathcal{K}(y^2) \mathcal{K}'(y^2) \right. \\
&\quad \left. - 4y^3 \hat{q}_\mu F(\hat{Q}) G(\hat{Q}) \left[\mathcal{K}(y^2) \mathcal{K}''(y^2) + \mathcal{K}'^2(y^2) \right] \right\} \\
&= \frac{v_F K_\mu}{8\pi^2} \int_{-\infty}^{\infty} dx \int_0^{2\pi} d\theta \left\{ \left[-4 \frac{\partial F(\hat{Q})}{\partial \hat{Q}_\mu} - 4 \hat{q}_\mu F(\hat{Q}) \right] G(\hat{Q}) \int_0^{\infty} y dy \mathcal{K}(y^2) \mathcal{K}'(y^2) \right. \\
&\quad \left. - 4 \hat{q}_\mu F(\hat{Q}) G(\hat{Q}) \int_0^{\infty} y^3 dy \left[\mathcal{K}(y^2) \mathcal{K}''(y^2) + \mathcal{K}'^2(y^2) \right] \right\}. \tag{82}
\end{aligned}$$

After integrating y out, we find

$$\int_0^{\infty} y^3 dy \left[\mathcal{K}(y^2) \mathcal{K}''(y^2) + \mathcal{K}'^2(y^2) \right] = - \int_0^{\infty} y dy \mathcal{K}(y^2) \mathcal{K}'(y^2) = \frac{1}{4}. \tag{83}$$

Therefore,

$$\begin{aligned}
\Lambda \frac{d\Sigma_{\text{nm}}(K)}{d\Lambda} &= \frac{v_F K_\mu}{8\pi^2} \int_{-\infty}^{\infty} dx \int_0^{2\pi} d\theta \left\{ \left[\frac{\partial F(\hat{Q})}{\partial \hat{Q}_\mu} + \hat{q}_\mu F(\hat{Q}) \right] G(\hat{Q}) - \hat{q}_\mu F(\hat{Q}) G(\hat{Q}) \right\} \\
&= \frac{v_F K_\mu}{8\pi^2} \int_{-\infty}^{\infty} dx \int_0^{2\pi} d\theta \frac{\partial F(\hat{Q})}{\partial \hat{Q}_\mu} G(\hat{Q}). \tag{84}
\end{aligned}$$

Formally, the fermion self-energy function can be expanded as

$$\frac{d\Sigma_{\text{nm}}(K)}{d \ln \Lambda} = C_1(-i\omega) + C_2 v_F k_x \tau^z + C_3 v_\Delta k_y \tau^x. \tag{85}$$

When $K_0 = \omega$ and $\hat{Q}_0 = v_F x$, we finally have

$$\begin{aligned}
C_1(-i\omega) &= \frac{v_F \omega}{8\pi^3} \int_{-\infty}^{\infty} dx \int_0^{2\pi} d\theta \frac{\partial F(\hat{Q})}{\partial v_F x} G(\hat{Q}) \\
&= \frac{2v_\Delta \omega}{N_f \pi^3 v_F} \int_{-\infty}^{\infty} dx \int_0^{2\pi} d\theta \frac{i(x^2 + \cos^2 \theta + (v_\Delta/v_F)^2 \sin^2 \theta) - 2x(ix - \cos \theta \tau^z + (v_\Delta/v_F) \sin \theta \tau^x)}{(x^2 + \cos^2 \theta + (v_\Delta/v_F)^2 \sin^2 \theta)^2} \mathcal{G}(x, \theta) \\
&= \frac{2(v_\Delta/v_F)}{N_f \pi^3} \int_{-\infty}^{\infty} dx \int_0^{2\pi} d\theta \frac{x^2 - \cos^2 \theta - (v_\Delta/v_F)^2 \sin^2 \theta}{(x^2 + \cos^2 \theta + (v_\Delta/v_F)^2 \sin^2 \theta)^2} \mathcal{G}(x, \theta) (-i\omega), \tag{86}
\end{aligned}$$

which directly leads to

$$C_1 = \frac{2(v_\Delta/v_F)}{N_f \pi^3} \int_{-\infty}^{\infty} dx \int_0^{2\pi} d\theta \frac{x^2 - \cos^2 \theta - (v_\Delta/v_F)^2 \sin^2 \theta}{(x^2 + \cos^2 \theta + (v_\Delta/v_F)^2 \sin^2 \theta)^2} \mathcal{G}(x, \theta). \tag{87}$$

C_2 and C_3 can be obtained similarly.

-
- [1] S. A. Kivelson, E. Fradkin, and V. J. Emery, *Nature* (London), **393**, 550 (1998).
[2] E. Fradkin, S. A. Kivelson, M. J. Lawler, J. P. Eisenstein, and A. P. Mackenzie, *Annu. Rev. Condens. Matter Phys.* **1**, 153 (2010).
[3] M. Vojta, *Adv. Phys.* **58**, 699 (2009).
[4] Y. Ando, K. Segawa, S. Komiyama, and A. N. Lavrov, *Phys. Rev. Lett.* **88**, 137005 (2002).
[5] V. Hinkov, D. Haug, B. Fauque, P. Bourges, Y. Sidis, A. Ivanov, C. Bernhard, C. T. Lin, and B. Keimer, *Science* **319**, 597 (2008).
[6] R. Daou, J. Chang, D. LeBoeuf, O. Cyr-Choiniere, F. Laliberte, N. Doiron-Leyraud, B. J. Ramshaw, R. Liang, D. A. Bonn, W. N. Hardy, and L. Taillefer, *Nature* (London) **463**, 519 (2010).
[7] M. J. Lawler, K. Fujita, Jinhwan Lee, A. R. Schmidt, Y.

- Kohsaka, Ch. K. Kim, H. Eisaki, S. Uchida, J. C. Davis, J. P. Sethna, and E.-A. Kim, *Nature* **466**, 347 (2010).
- [8] R. A. Borzi, S. A. Grigera, J. Farrell, R. S. Perry, S. J. S. Lister, S. L. Lee, D. A. Tennant, Y. Maeno, and A. P. Mackenzie, *Science* **315** 214 (2007).
- [9] T.-M. Chuang, M. P. Allan, J. Lee, Y. Xie, N. Ni, S. L. Budko, G. S. Boebinger, P. C. Canfield, and J. C. Davis, *Science* **327** 181 (2010).
- [10] J. A. Hertz, *Phys. Rev. B* **14**, 1165 (1976); A. J. Millis, *Phys. Rev. B* **48**, 7183 (1993).
- [11] J. Rech, C. Pepin, and A. V. Chubukov, *Phys. Rev. B* **74**, 195126 (2006).
- [12] K. Sun, B. M. Fregoso, M. J. Lawler, and E. Fradkin, *Phys. Rev. B* **78**, 085124 (2008).
- [13] M. Garst and A. V. Chubukov, *Phys. Rev. B* **81**, 235105 (2010).
- [14] M. A. Metlitski and S. Sachdev, *Phys. Rev. B* **82**, 075127 (2010).
- [15] C. J. Halboth and W. Metzner, *Phys. Rev. Lett.* **85**, 5162 (2000); W. Metzner, D. Rohe, and S. Andergassen, *Phys. Rev. Lett.* **91**, 066402 (2003).
- [16] V. Oganesyan, S. A. Kivelson, and E. Fradkin, *Phys. Rev. B* **64**, 195109 (2001).
- [17] M. Vojta, Y. Zhang, and S. Sachdev, *Phys. Rev. B* **62**, 6721 (2000); *Int. J. Mod. Phys. B* **14**, 3719 (2000).
- [18] E.-A. Kim, M. J. Lawler, P. Oretto, S. Sachdev, E. Fradkin, and S. A. Kivelson, *Phys. Rev. B* **77**, 184514 (2008).
- [19] Y. Huh and S. Sachdev, *Phys. Rev. B* **78**, 064512 (2008).
- [20] C. Xu, Y. Qi, and S. Sachdev, *Phys. Rev. B* **78**, 134507 (2008).
- [21] L. Fritz and S. Sachdev, *Phys. Rev. B* **80**, 144503 (2009).
- [22] C. Castellani, C. Di Castro, and M. Grilli, *Z. für Physik* **103**, 137 (1997).
- [23] S. Sachdev, M. A. Metlitski, Y. Qi, and C. Xu, *Phys. Rev. B* **80**, 155129 (2009).
- [24] J.-H. She and J. Zaanen, *Phys. Rev. B* **80**, 184518 (2009); S.-X. Yang, H. Fotsos, S.-Q. Su, D. Galanakis, E. Khatami, J.-H. She, J. Moreno, J. Zaanen, and M. Jarrell, *Phys. Rev. Lett.* **106**, 047004 (2011).
- [25] J. Orenstein and A. J. Millis, *Science* **288**, 468 (2000).
- [26] P. A. Lee, *Phys. Rev. Lett.* **71**, 1887 (1993); A. Durst and P. A. Lee, *Phys. Rev. B* **62**, 1270 (2000).
- [27] L. Taillefer, B. Lussier, R. Gagnon, K. Behnia, and H. Aubin, *Phys. Rev. Lett.* **79**, 483 (1997).
- [28] A. A. Nersesyan, A. M. Tsvetik, and F. Wenger, *Nucl. Phys. B* **438**, 561 (1994).
- [29] A. Altland, B. D. Simons, and M. R. Zirnbauer, *Phys. Rep.* **359**, 283 (2002).
- [30] A. W. W. Ludwig, M. P. A. Fisher, R. Shankar, and G. Grinstein, *Phys. Rev. B* **50**, 7526 (1994).
- [31] T. Stauber, F. Guinea, and M. A. H. Vozmediano, *Phys. Rev. B* **71**, 041406 (2005).
- [32] M. S. Foster and I. L. Aleiner, *Phys. Rev. Lett.* **77**, 195413 (2006).
- [33] R. Shankar, *Rev. Mod. Phys.* **66**, 129 (1994).
- [34] M. Chiao, R. W. Hill, Ch. Lupien, L. Taillefer, P. Lambert, R. Gagnon, and P. Fournier, *Phys. Rev. B* **62**, 3554 (2000).
- [35] J. Mesot, M. R. Norman, H. Ding, M. Randeria, J. C. Campuzano, A. Paramekanti, H. M. Fretwell, A. Kaminski, T. Takeuchi, T. Yokoya, T. Sato, T. Takahashi, T. Mochiku, and K. Kadowaki, *Phys. Rev. Lett.* **83**, 840 (1999).
- [36] G.-Z. Liu, W. Li, and G. Cheng, *Phys. Rev. B* **79**, 205429 (2009).
- [37] G.-Z. Liu and J.-R. Wang, *New J. Phys.* **13**, 033022 (2011).